RSC Advances

PAPER

View Article Online
View Journal | View Issue

Cite this: *RSC Adv.*, 2014, **4**, 53072

The quest for highly fluorescent chromophores: evaluation of 1*H*,3*H*-isochromeno[6,5,4-*mna*]xanthene-1,3-dione (CXD)†

Roza Al-Aqar, Daniel Avis, Andrew C. Benniston* and Anthony Harriman

Received 3rd September 2014
Accepted 2nd October 2014

DOI: 10.1039/c4ra09728a

www.rsc.org/advances

Photophysical properties of the strongly fluorescent dye, 1*H*,3*H*-isochromeno[6,5,4-*mna*]xanthene-1,3-dione (**CXD**), are reported. This highly planar, rigid dye absorbs at around 420 nm, which is ideal for excitation with a blue laser diode, and is extremely stable towards prolonged illumination. Under near-UV excitation, the dye readily sensitises free-radical polymerisation, forming a plastic film with excellent optical transparency. Weakly structured emission is observed with a small Stokes' shift and remains essentially insensitive to changes in solvent polarity. For example, in tetrahydrofuran the fluorescence quantum yield is 0.96 while the excited-singlet state lifetime is 7.4 ns. Quantum chemical calculations provide further insight into the electronic nature of the dye in solution.

Introduction

Fluorophores are ubiquitous in natural systems such as flora and have found their way into numerous man-made objects such as flat-screen monitors,[1] OLED devices,[2] banknotes,[3] artificial whiteners[4] and clothing.[5] Complementary developments in data processing and spectroscopic instrumentation have widened the scope for fluorescent sensors, allowing routine measurements to be made at the single-molecule level. Even though there is a plethora of highly emissive dyes, the quest to discover and characterise new fluorophores remains an important and topical subject, and is driven by both commercial and scientific interests. It is desirable that the fluorophore can be prepared in a few short steps from readily available sources and be purified without the need for over-elaborate chromatographic separation. The capability to easily functionalise the fluorophore at multiple sites is also a highly attractive trait.[6] To be a successful fluorophore, a number of photophysical and photochemical factors are requisite; namely, (i) a high fluorescence quantum yield, (ii) a low triplet yield, (iii) structured absorption/fluorescence profiles, (iv) a non-negligible, but not too large, Stokes' shift and (v) robustness on prolonged light exposure.[7] In the search for a new dye system with many of these outlined characteristics, the compound **CXD** (Fig. 1) was identified from critical scrutiny of the literature.[8–11] It might be noted that the anhydride subunit provides the necessary functionality by which to moderate the physiochemical properties of this class of dye. Further substitution can be attempted at the distal phenoxy-like ring, if required.

The limited data available in the literature hints at the possibility of an unusually high fluorescence probability, but no fluorescence quantum yield or excited-state lifetime have been reported. In addition, the planarity of the **CXD** ring system and its inherent simplicity suggested to us that the compound might be robust to photodegradation pathways. This is important because the advent of cheap, high powered laser diodes emitting in the near-UV region has created new opportunities for devising photochemical protocols based around stable dyes that absorb in this spectral window. As a test system, **CXD** has

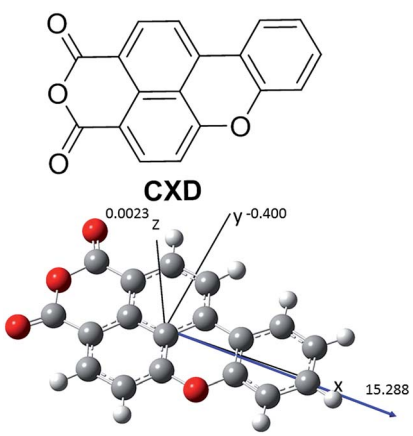

Fig. 1 Illustration of **CXD** (top) and its energy-minimised structure in MeCN showing the direction and value of the computed ground-state dipole moment vectors (bottom).

Molecular Photonics Laboratory, School of Chemistry, Newcastle University, Newcastle upon Tyne, NE1 7RU, UK. E-mail: a.c.benniston@ncl.ac.uk; Fax: +44 191 222 6929; Tel: +44 191 222 5706

† Electronic supplementary information (ESI) available: Computer calculated structures and absorption spectrum and additional UV-vis spectra. See DOI: 10.1039/c4ra09728a

been used as a blue-light photo-initiator[12] for the polymerisation of methyl methacrylate (Scheme 1).

Results and discussion

Synthesis

Prior work[8–11] has described the preparation of **CXD** and several close derivatives, but very little photophysical data were given. No electrochemical, physicochemical or theoretical data have been reported. We followed the generic synthetic route, making small modifications to optimise the overall efficacy and noting the appearance and chemical shifts for the $^{1}H/^{13}C$ NMR spectra. Displacement of the chlorine atom from **1** enables introduction of the nitrophenoxy group by way of a copper-catalysed mechanism, affording **2** as an orange powder. The small difference in the C=O groups was evident in the ^{13}C NMR spectrum which showed two resonances at $\delta = 160.91$ and 160.07 ppm. Subsequent reduction of the nitro group to the corresponding amine proceeded smoothly, although the diazonium-based ring annulation reaction to form **CXD** was problematic at first. The target compound was isolated as a yellow solid that was found to be reasonably soluble in most common organic solvents. Indeed, NMR studies showed the absence of aggregation at mM concentrations.

Computer calculations

The computed gas-phase structure for **CXD**, as determined by DFT using the B3LYP functional and the 6-311G^{++} basis set (Fig. 1), confirmed the compound to be essentially planar. Additional calculations were performed by placing the compound in a solvent reservoir. Calculated bond lengths are as expected for such an aromatic compound (see ESI†). The identification and spatial location of the HOMO and LUMO are in line with chemical intuition, while the gas-phase energy difference $E_{HOMO} - E_{LUMO}$ is calculated as being 3.33 eV for the energy-minimised geometry. Values for energies of the HOMO/LUMO where a solvent continuum model was applied are collected in Table 1. As might be expected, there is small increase in energy for both HOMO and LUMO relative to the vacuum, with the more polar solvents having the greater effect.

The electron density map for **CXD** is far more informative (Fig. 2A), however, revealing appreciable charge density build-up at the naphthalic anhydride segment of the dye. The region of lowest electron density is associated with the phenoxy-like subunit. As a result, **CXD** possesses an appreciable ground-state dipole moment, which is essentially long-axis polarised (Fig. 1). Dipole moments calculated in a solvent bath increase slightly in more polar solvents. The energy-minimised structure for the radical anion of **CXD** remains similar to that of the ground state. Bond length changes are associated with the naphthalic anhydride group, but do not alter greatly for the distal benzene ring (see ESI†). The electron density map compiled for **CXD**$^{-\bullet}$ (Fig. 2B) is fully consistent with an electron residing mainly at the naphthalic anhydride group. A comparable calculation performed on the **CXD**$^{+\bullet}$ predicts a planar geometry for the one-electron oxidised species with the positive charge being essentially localised at the phenoxy-like subunit (Fig. 2C).

Table 1 DFT computer calculated parameters using Gaussian 09 (ref. 13) and an IEPCFM solvent mode[a]

Solvent	E_{HOMO}/eV	E_{LUMO}/eV	Dipole moment/D
None	−6.523	−3.193	10.8
THF	−6.391	−3.151	14.5
DMSO	−6.366	−3.148	15.3
MeCN	−6.368	−3.148	15.3
Toluene	−6.440	−3.159	12.8
MeOH	−6.369	−3.149	15.3
Benzene	−6.444	−3.161	12.7

[a] B3LYP 6-311G^{++} basis set.

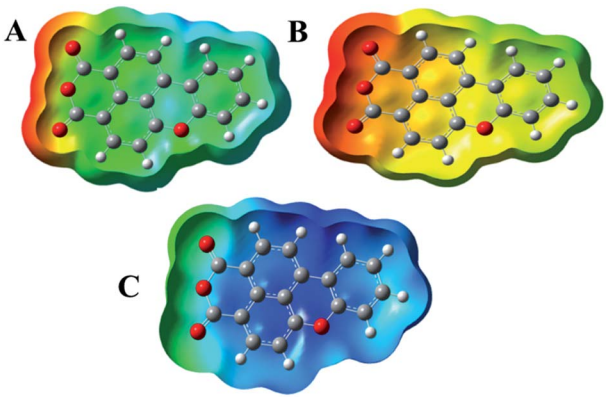

Fig. 2 DFT calculated electron density distribution for CXD (A), CXD$^{-\bullet}$ (B) and CXD$^{+\bullet}$ (C) in a MeCN solvent continuum model.

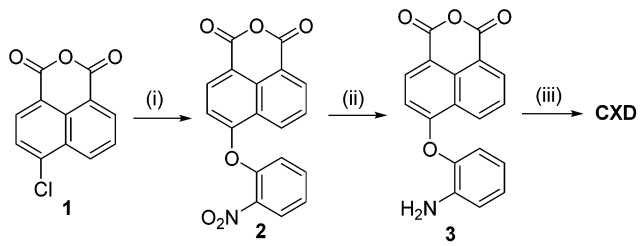

Scheme 1 Reagents and conditions: (i) KOH, Cu powder, 2-nitrophenol, DMF, reflux. (ii) Fe powder, acetic acid, reflux. (iii) Acetic acid, $NaNO_2$, 0 °C, $CuSO_4$ (aq), reflux, 30 min.

Electrochemistry

The redox behaviour of **CXD** in solution was evaluated using cyclic voltammetry in dried tetrahydrofuran (THF) and using tetrabutylammonium tetrafluoroborate (TBATFB) as background electrolyte. Upon oxidative scanning, an irreversible wave was observed with a peak centred at +1.65 V *vs.* SCE, which suggests that the radical cation of **CXD** is prone to decomposition. It is feasible that this radical cation undergoes proton loss, since similar behaviour is known for certain xanthene derivatives.[14] The reductive portion of the voltammogram was

dominated by a reversible, one-electron wave centred at −1.21 V (ΔE = 60 mV) *vs.* SCE. In view of the computer calculations and taking due account of previous work with relevant anhydrides,[15] we believe that generation of the radical anion corresponds to attachment of an electron at the naphthalic anhydride subunit. It is worth noting that the reduction potential for **CXD** is comparable to those of common electron acceptors such as 1,4-dicyanonaphalene and 1,4-dinitrobenzene.[16]

Absorption and fluorescence

Localised electronic transitions for the **CXD** chromophore were evident from its absorption spectrum recorded in THF (Fig. 3), which is red-shifted compared to benzo[*kl*]xanthene[17] and has features similar to naphthalic anhydride.[18] The absorption profile below 350 nm comprises a narrow, intense band centred at 270 nm and a weaker broad, but slightly structured, band centred at around 320 nm. The main absorption features are located at λ_{max1} = 420 nm (ε = 17 600 M^{-1} cm^{-1}) and λ_{max2} = 441 nm (ε = 14 500 M^{-1} cm^{-1}). There is also sign of a slight shoulder (~400 nm) to the high energy side of the main peak. This shoulder is far more prominent in non-polar solvents, such as toluene or diethyl ether, where the two main peaks are better defined (ESI† & Table 2). A TD-DFT calculated absorption spectrum for **CXD** in THF matches reasonably well with the observed spectrum (see ESI†) and indicates that the first-allowed absorption transition is located at 413 nm with an oscillator strength of 0.47. Essentially the main absorption feature is associated with the HOMO to LUMO electronic transition. There is a notable n–π* contribution to the high energy band located at 270 nm.

Intense emission is observed for an air-equilibrated THF solution of **CXD**, the fluorescence quantum yield (ϕ_{FLU}) being 0.96 and the excited-singlet state lifetime (τ_s) being 7.4 ns. Spectral deconstruction into Gaussian-shaped components indicates the lowest-energy absorption transition has an accompanying vibronic envelope corresponding to a group of modes centred at around 1230 cm^{-1}. Absorption is considered to correspond to Franck–Condon excitation, for which the 0,0 transition is located at 22 545 cm^{-1} by virtue of the spectral deconstruction. In contrast, spectral deconstruction of the emission profile requires the presence of two vibronic modes, corresponding to averaged values of 1145 and 1815 cm^{-1}. This leads to poor mirror symmetry between absorption and fluorescence profiles. Even so, there is good agreement of the radiative rate constant (k_{RAD} = 1.2 × 10^8 s^{-1}) calculated on the basis of the Strickler–Berg expression[19] (ESI†) and the experimental value ($k_{RAD} = \phi_{FLU}/\tau_s$) (Table 2). The emission 0,0 transition is located at 21 365 cm^{-1}, giving rise to a modest Stokes' shift of 1180 cm^{-1}.

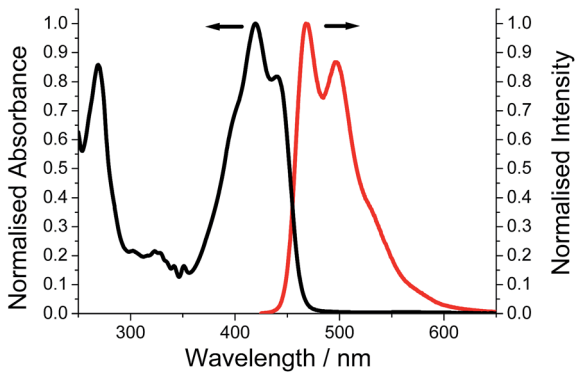

Fig. 3 Room temperature normalised absorption spectrum (black) and fluorescence spectrum (red) for **CXD** in THF.

Table 2 Collected photophysical parameters recorded for **CXD** in a small range of solvents at room temperature

Solvent	λ_{max} nm	ε_{max} M^{-1} cm^{-1}	λ_{em}/nm	ϕ_{FLU}	τ_s/ns	k_{RAD} 10^8 s^{-1}	k_{NR} 10^6 s^{-1}
THF[a]	420	17 600	467	0.96	7.4	1.3	5.1
	441	14 500	497				
MeCN	423	14 900	474	0.94	8.1	1.1	7.4
	443	12 800	500				
Toluene	424	16 200	467	0.95	7.7	1.2	6.8
	447	13 200	497				
DEE[b]	418	14 900	460	0.96	8.7	1.1	4.9
	440	12 000	490				
PC[c]	427	17 600	476	0.96	7.4	1.3	5.1
	445	17 200	503				

[a] Tetrahydrofuran. [b] Diethyl ether. [c] Propylene carbonate.

The quantum chemical calculations indicate that the molecular dipole moment increases by only *ca.* 0.8 D following excitation in THF, and this is consistent with the very limited effect of solvent polarity on the magnitude of the Stokes' shift (see below). Interestingly, the relaxed excited-singlet state reached *via* Franck–Condon excitation repositions the excess negative charge associated with internal charge transfer around the imide unit. For example, the ground-state molecule directs much of this excess charge to the carbonyl O atoms, these being very slightly disparate because of the bridgehead oxygen atom in the central ring. The relaxed excited-singlet state tends to offset some of this excess charge to the bridging O atom, such that the imide-based terminal presents a well-defined negative surface that might be suitable for selective binding to substrates and/or protein residues.

Photophysical properties measured for **CXD** in several solvents are collected in Table 2. Despite the subtle alterations to the shape of the fluorescence spectra with solvent, the lack of any correlation between the emission peak maximum (λ_{EM}) and a polarity function is consistent with the excited state possessing a dipole moment comparable to that of the ground state. Furthermore, fluorescence quantum yields are close to unity and constant across the series; the small variations in τ_s are attributed to perturbations in the non-radiative rate constants ($k_{NR} = 1/\tau_s - k_{RAD}$). There appears to be no simple correlation between k_{NR} and, for example, the polarity of the solvent (*e.g.*, THF *vs.* PC). The important point from this study is that emission is almost quantitative in solution at room temperature. Closely comparable emission spectral profiles were observed in the solid state after dispersal of the dye in thin plastic films of poly(methylmethacrylate) or silicone rubber. Furthermore, the

pure solid shows quite strong green fluorescence under near-UV (*i.e.*, 365 nm) illumination.

Given the extremely high fluorescence quantum yield, it follows that triplet formation must be very inefficient. No phosphorescence could be detected in an optical glass formed by freezing methyltetrahydrofuran to 77 K even in the presence of 50 v/v of iodoethane as an external heavy-atom perturber. The relevant Stern–Volmer plot for addition of iodoethane to **CXD** in THF at room temperature exhibits pronounced positive deviation from linearity, indicating formation of a non-emissive complex as well as dynamic quenching. From time-resolved emission studies, the bimolecular rate constant for the dynamical quenching component is derived to be *ca.* 3×10^6 M^{-1} s^{-1}. Thus, intersystem crossing within **CXD** seems relatively insensitive to spin–orbital perturbation. The TD-DFT calculations predict an energy level for the first-allowed triplet state of around 2.08 eV (611 nm), corresponding to a splitting of the S_1–T_1 levels of around 0.92 eV. Although the absolute energies cannot be relied on, such calculations often produce useful S_1–T_1 splittings. If so, the ineffective intersystem crossing process can be attributed, at least in part, to the large S_1–T_1 energy gap.

Photochemical stability

To be regarded as a universally viable fluorophore, the photochemical stability of **CXD** in both the solid state and in fluid solution must be extraordinarily high. There is a complete scarcity of literature information on this point but the low triplet yield alluded to above might be taken as indicative of the unimportance of problems related to singlet molecular oxygen side reactions. Indeed, solutions of **CXD** prepared in various air-equilibrated solvents were irradiated with an unfiltered tungsten lamp (400 W), and absorption spectra were collected over a period of 3 h. Example spectra accumulated in propylene carbonate are illustrated by way of Fig. 4. The profile of the main absorption features remains unchanged during such irradiation and minor alterations in the absorbance level are considered to be insignificant. Thus, under these conditions, degradation of the dye is negligible. The same conclusion was reached in other solvents. As a rough guide, the turnover number for excitation of the dye exceeds 30 000 in propylene carbonate and, in this experiment, there is less than 2% loss of the chromophore. The presence of dissolved oxygen has no effect on the photo-stability levels. Furthermore, the golden yellow colour characteristic of solid **CXD** when left in direct sunlight over several days also remained unchanged. Such factors point to an unusually high level of photo-stability for this dye.

Light-initiated polymerisation

It is clear in light of the above discussion that **CXD** is highly fluorescent in both fluid and solid media. Separate work has shown that the dye is stable on prolonged storage both in light and in the dark, regardless of the local concentration of molecular oxygen. Cyclic voltammetry and quantum chemical studies are suggestive of the ability of **CXD** to enter into photochemical electron-transfer reactions as either donor or acceptor. Overall, such properties are ideal for a next-generation photo-initiator for *in situ* polymerisation, for which there is an ever-expanding market.[20] Consequently, trial experiments were conducted with a view to establishing the credibility of employing **CXD** to sensitise the room temperature polymerisation of methyl methacrylate.

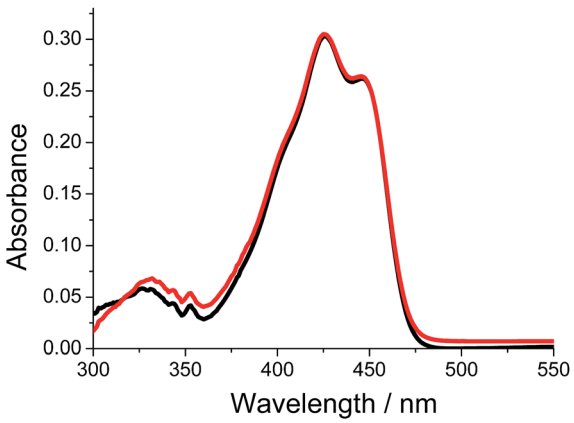

Fig. 4 Absorption spectra recorded for CXD in air-equilibrated propylene carbonate following irradiation with an unfiltered 400 W halogen lamp for 6 minutes (black curve) and 3 hours (red curve).

Initial studies showed that near-UV excitation of **CXD** in deoxygenated methanol containing the well-known initiator diphenyl iodonium chloride (**DPI**) at a concentration of 1 mM. Under illumination, **CXD** bleaches rapidly and the solution changes from bright yellow to transparent within a few minutes. It is interesting to note that there is no residual colouration after short irradiation periods. Although the reaction mechanism has not been probed in any detail, there is adequate literature information to suggest that the initial step involves electron transfer from the singlet-excited state of **CXD** to **DPI**, followed by rapid breakdown of the latter.[21] The resultant free radicals attack the chromophore, destroying conjugation and/or fragmenting the molecular backbone. Bleaching of **CXD** is irreversible, even in the presence of molecular oxygen. From a Stern–Volmer analysis of the fluorescence titration data collected for the addition of **DPI** to **CXD** in methanol solution, where the bimolecular quenching rate constant is derived to be 7×10^9 M^{-1} s^{-1}, it appears that the initial quenching probability is very high (*i.e.*, *ca.* 70%). In this case, there is no apparent indication for static quenching.

In a typical experiment, a solution of **DPI** (0.015 M) and methyl methacrylate (6.2 M) was prepared in methanol and thoroughly deoxygenated with a stream of dry N_2. Prolonged illumination ($\lambda > 360$ nm) did not cause polymerisation. Likewise, addition of **CXD** (20 μM) to the solution under anaerobic conditions had no effect on the viscosity but gave rise to a notable yellow colouration and intense fluorescence. Under illumination with near-UV light, this colouration disappeared and after a short period fluorescence could no longer be detected. The onset of polymerisation was readily followed by simply checking the viscosity of the solution. An illustration of

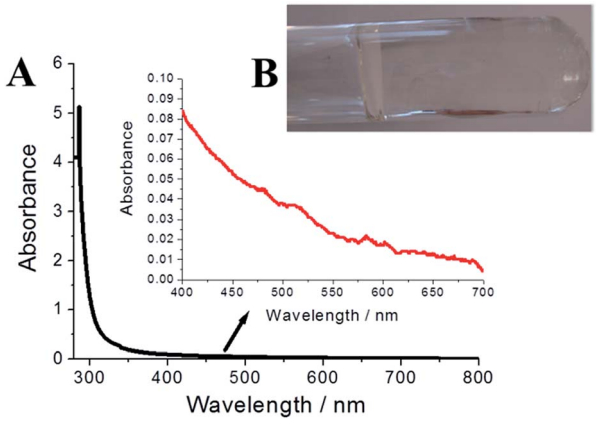

Fig. 5 Absorption spectrum for PMMA showing the Rayleigh scattering effect from the polymer (A), and a picture of the PMMA polymer in a glass tube.

the resultant highly viscous medium is shown in Fig. 5B. By eye, the matrix appears to be optically transparent although it is evident from the absorption spectrum (Fig. 5A) that there is some light scattering.

The photo-polymerisation studies described above give rise to a soft organo-gel that retains a high fraction of methanol within the matrix, although the viscosity is very high. Experiments confirmed that adventitious dyes are readily accommodated within the gel simply by equilibrating a concentrated solution of dye with the preformed gel. Several different dyes could be assimilated into the matrix in this fashion. In an attempt to probe the molecular environment within the gel, the polarity-sensitive probe **JBD** (ref. 22) was adsorbed into the polymeric matrix (Fig. 6). The absorption maximum characteristic of this latter dye depends on the local polarity, and also on the presence of acid. As an example, the absorption spectra recorded for **JBD** in dichloromethane (red), dibutyl ether (green) and methylcyclohexane (blue) are shown in Fig. 6. The observed spectrum for **JDB** dispersed in the preformed organo-gel is

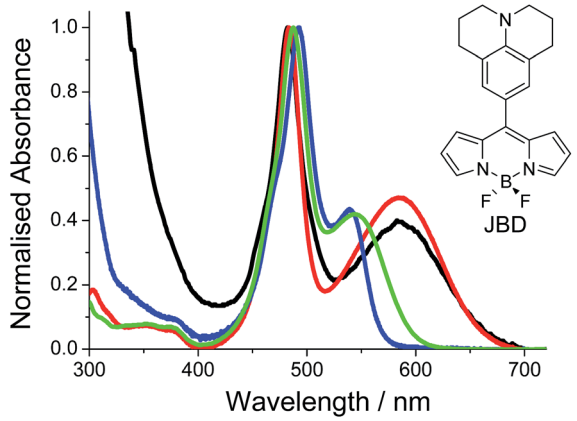

Fig. 6 Absorption spectra for proton/polarity sensitive probe in CH_2Cl_2 (red), dibutyl ether (green) and methyl-cyclohexane (blue) and when absorbed into the PMMA polymer (black).

consistent with a basic matrix, as might be expected if only a few ester moieties were inadvertently hydrolysed during the polymerisation step. The reported static dielectric constant (ε_s) for PMMA at room temperature is 3.5,[23] which is not dissimilar to that of dibutyl ether ($\varepsilon_s = 3.1$). It is noticeable that the absorption maximum noted for **JBD** in dibutyl ether is a poor match to that of the dye dispersed in the organo-gel. In fact, the latter corresponds more closely to that of dichloromethane, where ε_s is 8.93. Given the presence of methanol in the organo-gel, this results is not unreasonable.

Conclusions

We have demonstrated that the planar aromatic compound, **CXD**, is a highly successful candidate as an intensely fluorescent and photochemically robust dye. One very positive feature is the dye's near unity fluorescence quantum yield in a wide range of solvents. Certainly this feature bodes well the incorporation of **CXD** into molecular materials for applications in such areas as light emitting diodes; the anhydride offering a quick and easy site to functionalise the dye for such an application. As a blue-light photoinitiator **CXD** also looks to be a very viable candidate, especially using currently available laser diodes which emit at 405 nm, 457 nm and 462 nm.[24] The molar absorption coefficients for **CXD** at these three wavelengths are 13 200, 5000 and 2000 M^{-1} cm^{-1}. Evidently, at 405 nm the dye is tuned almost perfectly for laser excitation and would appear to be better candidate than naphthalimide and naphthalic anhydride derivatives discussed recently in the literature.[20]

Experimental

^{1}H-, ^{13}C-NMR spectra were recorded with either a Bruker-Avance-III 400 MHz spectrometer or a Bruker Avance 300 MHz spectrometer. Chemical shifts for ^{1}H- and ^{13}C-NMR spectra are referenced relative to the residual protiated solvent. IR spectra were recorded with Perkin Elmer Spectrum 100 FT-IR Spectrometer. Electronic absorption spectra were recorded using a Hitachi U3310 spectrophotometer and corrected fluorescence spectra were recorded using a Hitachi F-4500 spectrometer. Cyclic voltammetry experiments were performed using a fully automated HCH Instruments Electrochemical Analyzer and a three electrode set-up consisting of a glassy carbon working electrode, a platinum wire counter electrode and an SCE reference electrode. All studies were performed in deoxygenated THF containing TBATFB (0.2 M) as background electrolyte. Redox potentials were reproducible to within ±15 mV.

Computer calculations

Computational calculations were performed using a 32 bit version of Gaussian 09 (ref. 13) on a quadruple-core Intel Xeon system with 4 GB RAM. The calculations were run in parallel, fully utilising the multi-core processor. Energy minimisation calculations were monitored using Molden and run in parallel with frequency calculations to ensure optimised geometries represented local minima. Time-Dependent Density Functional

Theory (TD-DFT) calculations to simulate absorption spectra were carried out using B3LYP and the 6-31G(d) basis set (n states = 16) and an IEFPCM solvent model. The simulated absorption spectrum was read in GView and the peak half-width adjusted to match the observed spectrum.

Synthesis

All chemicals were purchased from commercial sources and used as received unless otherwise stated. Basic solvents for synthesis were dried using literature methods. Solvents for spectroscopic investigations were of the highest purity available.

Preparation of 1. 1,8-Naphthalic anhydride (9.5 g, 0.048 mol) and phosphoric acid (85%, 0.8 mL, 0.029 mol) were added to a pre-dissolved solution of sodium hydroxide (37.5 g, 0.938 mol) and water (900 mL, 49.945 mol). Chlorine gas, produced through the drop-wise addition of hydrochloric acid (210 mL, 2.557 mol) to potassium permanganate (31.86 g, 0.202 mol), was bubbled through the solution at room temperature for 3 hours. The precipitate which formed was filtered off, dried and recrystallized from ethanol to afford a white powder. Yield: 40%. Mp = 218–220 °C (literature 216–217 °C). ^{1}H NMR (300 MHz, $CDCl_3$); δ 8.70 (dd, $J^1 = 8.5$ Hz, $J^2 = 1.0$ Hz, 1H), 8.63 (dd, $J^1 = 7.3$ Hz, $J^2 = 1.0$, 1H), 8.48 (d, $J = 8.0$ Hz, 1H), 8.11 (d, $J = 8.0$, 1H), 8.06 (dd, $J^1 = 8.5$ Hz, $J^2 = 7.3$ Hz, 1H). ^{13}C NMR (75 MHz, $CDCl_3$); δ 160.40, 160.10, 138.52, 133.26, 132.52, 131.14, 130.77, 129.04, 128.65, 128.09, 120.05, 118.72. IR analysis; 3096 cm^{-1}, 1778 cm^{-1}, 1736 cm^{-1}, 775 cm^{-1}. UV-Vis analysis; λ_{max} = 338 nm (acetonitrile). R_f value: 0.57 (DCM).

Preparation of 2. 4-Chloro-1,8-naphthalic anhydride (5.1 g, 0.022 mol), potassium hydroxide (85%, 2.82 g, 0.043 mol), copper powder (0.2 g, 3.147 mmol) and 2-nitrophenol (98%, 6.61 g, 0.048 mol) were refluxed in DMF (110 mL, 1.421 mol) for 1 hour. After cooling, hydrochloric acid (20%, 100 mL, 1.22 mol), was added to the reaction mixture to form a precipitate. The precipitate was filtered off, dried and recrystallized from acetic acid to afford an orange powder. Yield: 40%. Mp = 264–266 °C (literature 268–269 °C). ^{1}H NMR (300 MHz, $CDCl_3$); δ 8.78 (dd, $J^1 = 8.4$ Hz, $J^2 = 1.1$ Hz, 1H), 8.62 (dd, $J^1 = 7.3$ Hz, $J^2 = 1.1$ Hz, 1H), 8.44 (d, $J = 8.3$ Hz, 1H), 8.28 (dd, $J^1 = 8.4$ Hz, $J^2 = 1.5$, 1H), 8.00 (d, $J^1 = 8.4$ Hz, $J^2 = 7.3$ Hz, 1H), 7.94 (t, $J = 7.7$ Hz, 1H), 7.66 (m, 2H), 7.06 (d, $J = 8.3$ Hz, 1H). ^{13}C NMR (75 MHz, $CDCl_3$); δ 160.91, 160.07, 158.86, 146.39, 141.73, 136.22, 134.42, 133.33, 131.42, 129.25, 127.81, 127.38, 126.60, 124.51, 122.93, 119.39, 113.70, 110.61. IR analysis; 3084 cm^{-1}, 1761 cm^{-1}, 1725 cm^{-1}, 1525 cm^{-1}, 1344 cm^{-1}, 1251 cm^{-1}, 1025 cm^{-1}. UV-Vis analysis; λ_{max} = 351 nm (acetonitrile). R_f value: 0.33 (DCM).

Preparation of 3. 4-(2-Nitrophenoxy)-1,8-naphthalic anhydride (2 g, 0.059 mol) and iron powder (0.83 g, 0.015 mol) were refluxed in glacial acetic acid (75 mL, 1.310 mol) for 1.5 hours. Water (225 mL) was then added to the reaction mixture to form a precipitate. The iron powder was removed and the precipitate was filtered off, washed with water and dried thoroughly to afford a yellow powder. Yield = 91%. Mp = 170–172 °C (171–174 °C literature). ^{1}H NMR (400 MHz, d_6-DMSO); δ 8.88 (d, $J = 7.6$ Hz, 1H), 8.61 (d, $J = 7.6$ Hz, 1H), 8.46 (d, $J = 8.2$ Hz, 1H), 7.96 (t, $J = 7.6$ Hz, 1H), 7.09 (t, $J = 8.1$ Hz, 1H), 7.04 (d, $J = 8.2$ Hz, 1H), 6.92 (d, $J = 8.1$ Hz, 1H), 6.83 (d, $J = 8.1$ Hz, 1H), 6.67 (t, $J = 8.1$, 1H), 5.16 (s, 2H). ^{13}C NMR (100 MHz, d_6-DMSO); δ 160.02, 160.10, 160.05, 140.81, 138.96, 135.09, 133.09, 131.35, 130.19, 126.89, 126.81, 122.98, 121.67, 118.59, 116.55, 116.45, 111.44, 109.01. IR analysis; 3473 cm^{-1}, 3375 cm^{-1}, 3080 cm^{-1}, 1767 cm^{-1}, 1729 cm^{-1}, 1578 cm^{-1}. UV-Vis analysis; λ_{max} = 358 nm (DMF). R_f value: 0.14 (DCM).

Preparation of CXD. 4-(2-Aminophenoxy)-1,8-naphthalic anhydride (1.5 g, 4.913 mmol) was dissolved in glacial acetic acid (35 mL, 0.611 mol) and cooled to 0 °C whilst being stirred. Pre-cooled hydrochloric acid (3 mL, 0.037 mol) and sodium nitrite solution (3.29 g, 0.046 mol in 12 mL of water) were added at 0 °C. Copper sulphate pentahydrate solution (5.08 g, 0.020 mol in 57 mL of water) was added after 1 hour, and the reaction mixture was refluxed for 30 minutes. The precipitate formed, after cooling, was then filtered washed with water and recrystallized from DMF. Appearance: yellow-orange powder. Yield: 60%. Mp 150–152 °C (156–159 °C literature). ^{1}H NMR (400 MHz, d_6-DMSO) δ 8.54 (d, $J = 8.0$ Hz, 1H), 8.49 (d, $J = 8.5$ Hz, 1H), 8.40 (d, $J = 7.4$ Hz, 1H), 8.31 (d, $J = 8.0$ Hz, 1H), 7.68 (t, $J^1 = 8.0$ Hz, $J^2 = 7.4$ Hz, 1H), 7.50 (m, 3H). ^{13}C NMR (100 MHz, d_6-DMSO) δ 161.20, 160.71, 156.57, 151.93, 135.78, 135.15, 134.69, 133.62, 132.80, 126.18, 125.32, 118.95, 118.89, 118.44, 116.69, 116.56, 110.62, 111.32, 111.03. IR analysis; 2969 cm^{-1}, 1759 cm^{-1}, 1723 cm^{-1}. UV-Vis analysis; λ_{max} = 425 nm (DMF). R_f value: 0.26 (DCM).

Photopolymerisation of methyl methacrylate

To a glass tube fitted with a suba-seal was added methyl methacrylate dissolved in MeOH (10 mL). The photoinitiator **CXD** (20 μM) dissolved in a small amount of propylene carbonate and diphenyl iodonium chloride (0.015 M) were added, and the solution was purged thoroughly with dry N_2 for 20 min. The glass tube was irradiated for set time periods with white light, which had been filtered through a water bath to remove IR radiation, from a 400 W halogen lamp. The progress of polymerisation was followed by visually monitoring the change in viscosity of the solution as the reaction proceeded.

Dye adsorption

A small amount of dye (~0.1 mg) was dissolved in $CHCl_3$ (10 mL) and a disc cut from the PMMA polymer was placed in the solution and left for 1 h. The disc was removed, washed with acetone and $CHCl_3$ to remove dye adhered to the surface and dried in air. For direct absorption the dye (~0.1 mg) was mixed with PMMA (~100 mg) pellets in $CHCl_3$ (2 mL) and sonicated for 5 minutes. The solution was poured onto a clean glass slide and the solvent allowed to evaporate.

Acknowledgements

We thank Newcastle University for financial support and a scholarship (RAA) from the Higher Committee for Education Development (HCED) in Iraq.

Notes and references

1 D. E. Mentley, *Proc. IEEE*, 2002, **90**, 453; S. M. Kelly, *Flat Panel Displays: Advanced Organic Materials*, Royal Society of Chemistry, 2000.

2 M. Zhu and C. Yang, *Chem. Soc. Rev.*, 2013, **42**, 4963.

3 A. Bruna, G. M. Farinella, G. C. Guarnera and S. Battiato, *Sensors*, 2013, **13**, 2515.

4 D. W. Rangnekar and P. V. Tagdiwala, *Dyes Pigm.*, 1986, **7**, 445; V. S. Patil, V. S. Padalkar and N. Sekar, *J. Fluoresc.*, 2014, **24**, 1077; H. Shi, H. Lui, Y. Ni, Z. Yaun, X. Zou and Y. Zhou, *BioResources*, 2012, **7**, 2582.

5 C. Qin, R.-C. Tang, B. Chen, D. Chen, X. Wang and G. Chen, *Fibers Polym.*, 2010, **11**, 193; H.-C. Chen and W.-H. Ding, *J. Chromatogr. A*, 2006, **1108**, 202.

6 D. Ding, K. Li, B. Lui and B. Z. Tang, *Acc. Chem. Res.*, 2013, **46**, 2441; J. Fan, M. Hu, P. Zhan and X. Peng, *Chem. Soc. Rev.*, 2013, **42**, 29.

7 J. R. Lakowicz, *Principles of Fluorescence Spectroscopy*, Springer, 2nd edn, 2004.

8 S. Tan, H. Yin, Z. Chen, X. Qian and Y. Xu, *Eur. J. Med. Chem.*, 2013, **62**, 130.

9 Q. Xuhong and R. Shengwu, *J. Chem. Eng. Data*, 1988, **33**, 528.

10 X. Qian, J. Cui and R. Zhang, *Chem. Commun.*, 2001, 2656.

11 M. Prickett, G. Singh and H. Vankayalapati, *Tetrahedron Lett.*, 2000, **41**, 2987.

12 P. Xiao, F. Dumur, M. Frigoli, B. Graff, F. Moret-Savary, G. Wantz, H. Bock, J. P. Fouassier, D. Gigmes and J. Lalevée, *Eur. Polym. J.*, 2014, **53**, 215.

13 M. J. Frisch, G. W. Trucks, H. B. Schlegel, G. E. Scuseria, M. A. Robb, J. R. Cheeseman, G. Scalmani, V. Barone, B. Mennucci, G. A. Petersson, H. Nakatsuji, M. Caricato, X. Li, H. P. Hratchian, A. F. Izmaylov, J. Bloino, G. Zheng, J. L. Sonnenberg, M. Hada, M. Ehara, K. Toyota, R. Fukuda, J. Hasegawa, M. Ishida, T. Nakajima, Y. Honda, O. Kitao, H. Nakai, T. Vreven, J. A. Montgomery Jr, J. E. Peralta, F. Ogliaro, M. Bearpark, J. J. Heyd, E. Brothers, K. N. Kudin, V. N. Staroverov, R. Kobayashi, J. Normand, K. Raghavachari, A. Rendell, J. C. Burant, S. S. Iyengar, J. Tomasi, M. Cossi, N. Rega, J. M. Millam, M. Klene, J. E. Knox, J. B. Cross, V. Bakken, C. Adamo, J. Jaramillo, R. Gomperts, R. E. Stratmann, O. Yazyev, A. J. Austin, R. Cammi, C. Pomelli, J. W. Ochterski, R. L. Martin, K. Morokuma, V. G. Zakrzewski, G. A. Voth, P. Salvador, J. J. Dannenberg, S. Dapprich, A. D. Daniels, Ö. Farkas, J. B. Foresman, J. V. Ortiz, J. Cioslowski and D. J. Fox, *Gaussian 09, Revision D.01*, Gaussian, Inc., Wallingford, CT, 2009.

14 A. Marcinek, J. Rogowski, J. Adamus, J. Gębicki and M. S. Platz, *J. Phys. Chem.*, 1996, **100**, 13539.

15 S. K. Lee, Y. Zu, A. Herrmann, Y. Geerts, K. Müllen and A. J. Bard, *J. Am. Chem. Soc.*, 1999, **121**, 3513.

16 G. J. Kavarnos, *Fundamentals of Photoinduced Electron Transfer*, VCH Publishers, Inc, 1993.

17 J. F. Muller, D. Cagniant, O. Chalvet, D. Lavalette, J. Kolc and J. Michl, *J. Am. Chem. Soc.*, 1974, **96**, 5038.

18 M. S. Alexiou, V. Tychopoulos, S. Ghorbanian, J. H. P. Tyman, R. G. Brown and P. I. Brittain, *J. Chem. Soc., Perkin Trans. 2*, 1990, 837.

19 S. J. Strickler and R. A. Berg, *J. Chem. Phys.*, 1962, **37**, 814.

20 P. Xiao, F. Dumar, B. Graff, D. Gigmes, J. P. Fouassier and J. Lalevée, *Macromolecules*, 2014, **47**, 601.

21 Using the photophysical and electrochemical data for **CXD** its excited state is a good photoreductant ($E_{D+/D*} \sim -1$ V *vs.* SCE) and there is easily enough driving force to reduce **DPI** which is known to decompose; see ref. 12.

22 A. C. Benniston, S. Clift and A. Harriman, *J. Mol. Struct.*, 2011, **985**, 346.

23 M. S. Frahn, L. H. Luthjens and J. M. Warman, *J. Phys. Chem. B*, 2004, **108**, 2839.

24 S. Nakamura, S. Pearton and G. Fasol, *The Blue Laser Diode: The Complete Story*, Springer, 2000; M. R. Krames, O. B. Shchekin, R. Mueller-Mach, G. O. Mueller, L. Zhou, G. Harbers and M. G. Craford, *J. Disp. Technol.*, 2007, **3**, 160.

